3D DISTRIBUTION OF PERLECAN WITHIN INTERVERTEBRAL DISC CHONDRONS SUGGESTS NOVEL REGULATORY ROLES FOR THIS MULTIFUNCTIONAL MODULAR HEPARAN SULPHATE PROTEOGLYCAN

A.J. Hayes[1] and J. Melrose[2,3,4,*]

[1] Bioimaging Research Hub, Cardiff School of Biosciences, Cardiff University, Cardiff CF10 3AX, Wales, UK
[2] Graduate School of Biomedical Engineering, UNSW Sydney, Sydney, NSW 2052, Australia
[3] Raymond Purves Bone and Joint Research Laboratories, Kolling Institute of Medical Research, Royal North Shore Hospital and The Faculty of Medicine and Health, The University of Sydney, St. Leonards, NSW 2065, Australia
[4] Sydney Medical School, Northern, Sydney University, Royal North Shore Hospital, St. Leonards, NSW 2065, Australia

Abstract

Perlecan is a modular, multifunctional heparan sulphate-proteoglycan (HS-PG) that is present in the pericellular and wider extracellular matrix of connective tissues. In the present study, confocal microscopy was used to study perlecan distribution within intervertebral disc chondrons. Perlecan immunolabel was demonstrated intracellularly and in close association with the cell nucleus within chondrons of both the annulus fibrosus (AF) and nucleus pulposus (NP). This observation is consistent with earlier studies that have localised HS-PGs with nuclear cytoskeletal components. Nuclear HS-PGs have been proposed to transport fibroblast growth factor (FGF)-1, FGF-2 and FGFR-1 into the cell nucleus, influencing cell proliferation and the cell-cycle. Perlecan has well-known interactive properties with FGF family members in the pericellular and extracellular matrix. Perinuclear perlecan may also participate in translocation events with FGFs. The glycosaminoglycan side chains of HS-PGs can modulate chromatin structure by regulating the access of transcription factors to DNA. These mechanisms are consistent with the distribution patterns identified here and previously reported for other HS-PGs, introducing a potentially-novel arena for perlecan in gene regulation. Whilst much is known of the structure and function of perlecan in the pericellular and extracellular matrix, very little is known of any intracellular forms of perlecan. The perlecan labelling patterns described here suggest the possibility of involvement of this HS-PG in an intracrine regulatory system. Future studies should further explore this possibility and the potential for this HS-PG as a novel therapeutic target.

Keywords: Perlecan, intracellular, heparan sulphate, intervertebral disc, Wnt signalling pathway, fibroblast growth factor-2, fibroblast growth factor receptor-1.

***Address for correspondence**: Prof J Melrose, Raymond Purves Bone and Joint Laboratories, Level 10, Kolling Institute of Medical Research, B6, Royal North Shore Hospital, St. Leonards, New South Wales 2065 Australia. Telephone number: +61 425 364 725 Email: james.melrose@sydney.edu.au

List of Abbreviations

3D	3 dimensional
ADAMTS	a disintegrin and metalloproteinase with thrombospondin motifs
AF	annulus fibrosus
AFM	atomic force microscopy
BMP	bone morphogenetic protein
CS	chondroitin sulphate
DAPI	4′,6-diamidino-2-phenylindole
DIC	differential interference contrast
DS	dermatan sulphate
ECM	extracellular matrix
FGF	fibroblast growth factor
FGFR	fibroblast growth factor receptors
GAG	glycosaminoglycan
GPC	glypican
HIF-1α	hypoxia inducible factor-1α
HS	heparan sulphate
HSPG2	perlecan
IL-1β	interleukin-1β
IVD	intervertebral disc

MMP-1,2 and 9	matrix metalloproteinase-1,-2 and -9
NCAM	neural cell adhesion molecule
NF-κB	nuclear factor kappa-light-chain-enhancer of activated B cells
NP	nucleus pulposus
PBS	phosphate buffered saline
PCM	pericellular matrix
PDGF	platelet-derived growth factor
PG	proteoglycan
PHDs	prolyl hydroxylases
ROI	region of interest
SDC-1,2 & 4	syndecan-1, -2 and -4
SEA	sperm protein-enterokinase agrin
TGF-β	transforming growth factor β
TNF-α	tumour necrosis factor α
VEGF	vascular endothelial growth factor
VEGFA	vascular endothelial growth factor A
VEGFR-2	vascular endothelial growth factor receptor-2
Wnt	wingless-related integration site

Introduction

Perlecan (*HSPG2*) a large modular, multifunctional HS or HS/CS hybrid PG has a pericellular or extracellular tissue distribution in a number of connective tissues (Melrose *et al.*, 2006; Melrose *et al.*, 2008a; Smith *et al.*, 2010). It is a 5-domain, cell-regulatory PG displaying homology with the SEA domain, laminin G domains, NCAM-like immunoglobulin repeats, epidermal growth factor-like modules (Cohen *et al.*, 1993; Murdoch *et al.*, 1992; Noonan *et al.*, 1991) and is capable of interacting with a diverse range of growth factors, morphogens, ECM components, proteases and protease inhibitory proteins (Melrose *et al.*, 2008a; Melrose *et al.*, 2006). Functions ascribed to perlecan include sequestration of a number of different growth factors, with perlecan acting as a co-receptor: matrix stabilisation; modulation of tissue fibrosis through control of platelet function; promotion and inhibition of angiogenesis (Lord *et al.*, 2014); assembly of the neuromuscular junction controlling muscle activity; assembly and stabilisation of the basement membrane and blood vessel vasculature (Breitkreutz *et al.*, 2013; Nakamura *et al.*, 2019) and regulation of collagen fibrillogenesis (Kvist *et al.*, 2006). Perlecan is also associated with the development of a number of tumours through its ability to promote angiogenesis, but also contains bioactive anti-angiogenic peptide modules within domain V that antagonise VEGFA-VEGFR-2 interactions and the interaction of endothelial cells with α2β1 integrin, inhibiting tube formation (Lord *et al.*, 2014).

AFM studies have shown that pericellular perlecan has biomechanical properties in articular cartilage through interaction with type VI collagen, a major component of the chondron basket-like structure, and it is therefore likely to play similar roles in IVD function (McLeod *et al.*, 2013; Wilusz *et al.*, 2012). Perlecan co-localises with elastic microfibrils in the AF and imparts compliancy to this collagen-rich tissue (Hayes *et al.*, 2011b). Elastic microfibrils also convey mechanosensory cell signalling properties to the strings of cells interconnected by perlecan in the AF (Hayes *et al.*, 2011a). Pericellular perlecan plays a cytoprotective role in cartilage chondrons and would convey similar beneficial properties to IVD cells, providing protection from the harsh biomechanical environment encountered in the disc during gait (Wilusz *et al.*, 2012). Perlecan is also involved in the co-acervation of tropoelastin, as part of the elastic microfibril assembly process at the cell surface in the AF (Hayes, 2011a). As stated, perlecan is a multifunctional PG and interacts with collagen types VI (Hayes *et al.*, 2016) and type XI within the PCM compartment (Smith and Melrose, 2019) to stabilise the chondron structure. It also interacts with a variety of structural and cell-adhesive glycoproteins at the cell surface and within the wider ECM (Gomes *et al.*, 2004; Knox and Whitelock, 2006; Melrose *et al.*, 2008a and b; Melrose *et al.*, 2006). Perlecan has cell-directive properties, promoting the proliferation and differentiation of disc cells through its ability to act as a low affinity co-receptor for a number of growth factors including members of the FGF family, VEGF, PDGF and BMP-2 and 4 (Lord *et al.*, 2014; Whitelock *et al.*, 2008). Perlecan facilitates complex formation between FGF family members and their FGFRs resulting in activation of the FGFRs, which directs cell signalling events that drive tissue expansion during IVD development (Lord *et al.*, 2014; Melrose *et al.*, 2003; Whitelock *et al.*, 2008). Interestingly, some HS-PG family members have been shown to be shuttled into the nucleus of cells where they interact with nuclear FGF-1, 2 and FGFRs to regulate the cell-cycle, mitosis and cellular proliferation (Kovalszky *et al.*, 2014). Of relevance, perlecan has been shown to exist as a nuclear component in neurons and glial cells where it has been proposed to modulate astrocyte activity during astrogliotic events accompanying traumatic brain injury (Leadbeater *et al.*, 2006).

During studies on the IVD, many research groups have characterised a number of roles for PCM and ECM perlecan in the pathobiology of the IVD (Gomes *et al.*, 2004; Kirn-Safran *et al.*, 2009; Knox *et al.*, 2006; Melrose *et al.*, 2008a). In one of the studies, the presence of intracellular perlecan immunolabelling was identified within IVD tissues. The present study followed up on these initial observations, by characterising the 3D distribution and organisation of perlecan within IVD chondrons to examine the potential roles it plays in the regulation of IVD cells. The rationale for this study originated from earlier observations on nuclear HS-PGs in a number of cell types and the documented roles for perlecan as an instructive PG that directs many aspects of the metabolism of connective tissue cells, ECM organisation and stabilisation. There was particularly interested in the potential roles that perlecan may play in the control of IVD-cell behaviour through direct effects on nuclear organisation and gene regulation, as this might represent an area to target in future interventional therapeutic measures.

Consequently, the aim was to map the 3D labelling patterns of perlecan both within and outside of the cell in the different IVD tissues and to review potential functional implications of these labelling patterns on IVD-cell metabolism, based on published information on this interesting multifunctional HS-PG. To this end laser scanning confocal microscopy was used to evaluate the 3D distribution and organisation of perlecan in histological sections of ovine IVD using an antibody to perlecan domain IV. Here, stacks of serial optical sections are presented, taken at approximately 0.5 μm steps through the full volume of individual disc chondrons from AF and NP, as well as 3D models of the reconstructed stacks to provide accurate spatial information of perlecan distribution and organisation within the different discal regions. Furthermore, compelling evidence is provided to suggest the intracellular localisation of perlecan.

Materials and Methods

Rat monoclonal anti-perlecan domain-IV (A7L6) (ab2501) antibody was obtained from Abcam, Cambridge, UK. Rabbit polyclonal anti-type VI collagen antisera (VIb) was a gift from Dr Shirley Ayad, Manchester University (Ayad *et al*., 1989). Vectorshield tissue mountant containing DAPI was purchased through Vector Laboratories, Peterborough, UK.

Intervertebral disc tissues

6, 2-year old merino wether sheep (castrated males) from a single flock were obtained for these studies from a local animal sale yard. Sheep were sacrificed with an overdose of pentobarbital and lumbar spinal IVD segments (L1L2 to L6L7) were excised. Individual IVDs containing segments of the superior and inferior vertebral bodies still attached were excised using a bone saw and the IVDs were fixed *en bloc* in 10 % v/v neutral buffered formalin and then decalcified. This processing ensured that swelling artefacts were minimised in the IVD specimens. An unconstrained IVD fixation/decalcification results in a severe distortion in authentic tissue architecture due to artefactual swelling (Melrose *et al*., 2008c). Fixed/decalcified 5 mm thick tissue slabs were cut and embedded in paraffin wax and vertical mid-sagittal microtome sections (7 μm) were prepared for confocal analysis. The animals used were skeletally mature, had been treated with a broad range anti-parasitic program, were bright eyed, and had good skeletal form with appropriate muscle to fat proportions. They also displayed correct ambulation, while their feeding and flocking behaviour were unremarkable. Therefore, the sheep were fit and healthy. All animal welfare and ethics for this work were approved by the University of Sydney Animal Care and Ethics Committee under ethics approval A45/6-2011/3/5544.

Histological processing and immunohistochemistry

Tissue sections were deparaffinised in graded ethanol washes to water. IVD sections were stained for 10 min with 0.04 % (w/v) toluidine blue in 0.1 mol/L sodium acetate buffer, pH 4.0 followed by a 2-min counterstain in 0.1 % (w/v) fast green FCF. Sections were also stained in Mayer's haematoxylin (5 min), rinsed in tap water blued in Scott's blueing solution (1 min) and counterstained in 0.0001 % (w/v) eosin (5 min). Sections were washed for 3 × 5 min in 0.1 mol/L PBS at pH 7.4 containing 0.01 % TWEEN 20 (Merck, Dorset, UK), which was also used as a diluent for all immuno-reagents. Sections were either labelled for perlecan alone or were dual labelled in sequence for perlecan and type VI collagen. For perlecan localisations, non-specific antibody binding was blocked using donkey serum (Agilent Technologies, Stockport, UK) and, for type VI localisations, goat blocking serum (Agilent Technologies) was used, both at 1 : 20 dilution for 30 min at room temperature. Perlecan was immunolocalised overnight at 4 °C using a rat anti-perlecan domain IV (MAb A7L6) antibody (Abcam) at 1 : 50 dilution; type VI collagen was immunolocalised for 2 h at room temperature using a rabbit anti-type VI collagen polyclonal antibody (2 μg/mL) – a gift from Dr Shirley Ayad, Manchester University (Ayad *et al*., 1989). After labelling, sections were washed in PBS, as described, and primary antibody binding detected with an Alexa 594-conjugated donkey anti-rat secondary antibody for perlecan (red fluorescence) (ThermoFisher Scientific, Loughborough, UK), and an Alexa 488-conjugated goat anti-rabbit secondary antibody for type VI collagen (green fluorescence) (ThermoFisher Scientific), both used at 1 : 200 dilution for 1 h at room temperature. After washing, tissue sections were mounted under glass histology coverslips using Vectashield mountant containing DAPI to counterstain the cell nuclei (blue fluorescence) (Vector Laboratories). Negative-control slides were similarly processed but the primary perlecan antibody was omitted or was replaced with an irrelevant antibody. All controls showed no non-specific antibody binding.

Confocal laser scanning microscopy

Fluorescently-labelled IVD tissue sections were scanned on a Leica TCS SP2 AOBS laser scanning confocal microscope (Leica, Heidelberg, Germany) using 40 × and 63 × oil-immersion objectives. To eliminate spectral bleed-through between fluorescent dyes, samples were scanned sequentially using appropriate excitation and emission settings for DAPI (Ex. max., 359 nm; Em. max., 461 nm; blue nuclear fluorescence) and Alexa 594 (Ex. max., 594 nm; Em. max., 618 nm; red perlecan fluorescence) or DAPI, Alexa 594 and Alexa 488 (Ex. max., 488 nm; Em. max., 510 nm; green type VI collagen fluorescence) for dual-immunolocalisation experiments. Z-stacks of 8-bit 'optical sections' (512 × 512 pixels) were taken through the full thickness of the IVD tissue sections

at a spacing of approximately 0.6 μm increments using Leica Confocal Software (Leica, Heidelberg, Germany) and used to prepare gallery images of the perlecan and DAPI localisations and videos of these sequential image sequences were also prepared.

3D reconstruction of confocal Z-stacks

Confocal image datasets were also imported into Imaris for Cell Biologists software (Bitplane, Oxford Instruments, Zurich, Switzerland) for 3D processing and fluorescent localisation analysis. To conceptualise the fluorescent labelling patterns in 3D space, Z-stacks were modelled using maximum intensity and surface coding reconstruction algorithms. To contextualise the 3D-labelling pattern of perlecan in relation to type VI collagen, overlay images were created in which the type VI collagen channel was rendered semi-transparent with respect to the underlying perlecan channel (red).

Results

Vertical sections of ovine IVDs stained with toluidine blue-fast green, which was used to delineate PG localisation (Fig. 1**a**,**c**), and haematoxylin and eosin (Fig. 1**b**,**d**), used to reveal cellular morphology, indicate the main ROIs in the present study, *i.e.* outer AF and NP. Representative ROIs of NP and AF are indicated using the boxed areas shown. A schematic figure of a representative chondron containing 2 disc cells has been provided to clarify the major structural features of a chondron using terminology proposed by Pritzker and Aigner (2010) (Fig. 1**e**).

Sequential analysis of optical sections from confocal Z-stacks revealed the spatial organisation of perlecan within chondrons of the AF and NP of the IVD (Fig. 2). Perlecan label was distributed diffusely within the territorial matrix compartment but was highly prominent pericellularly, forming a well-defined zone around disc cells (Fig. 2). Video sequences through the Z-stacks, depicted in Fig. 2, are also presented as supplementary videos to better convey perlecan's 3D distribution within the chondron in the 2 distinct discal regions. In selected sections, perlecan immunofluorescence appeared to extend from the pericellular matrix into the lacunar space occupied by the disc cell, often manifesting as intense punctate foci (Fig. 3). Higher magnification images (Fig. 4) showed a distinct band of perlecan immunofluorescence, surrounding the cell that was in close association with the cell nucleus and a thin perlecan-negative discontinuity separated this band of fluorescent label from an adjacent outer zone of perlecan positive matrix further enveloping the cell. Dual-labelling experiments (see below) indicated that this discontinuity within the chondron capsule was occupied by collagenous ECM material, particularly type VI collagen. Intense foci of perlecan label were also evident throughout the territorial matrix (Fig. 4**a**,**b**). These features are explained in Fig. 1**e**.

A superficial section taken through a single chondron within the NP demonstrated the presence of large perlecan-positive vesicular structures; whilst deeper sections within the image stack, taken through the chondrocyte itself, showed the presence of punctate foci, characteristic of intracellular vesicles, that were closely associated with the cell nucleus (Figs. 5, 6). In many of the cells examined, pericellular perlecan enveloped the cell nucleus so tightly that it was difficult to identify the lacunar space; however, in some examples the lacunar margins could be clearly delineated when the cell had artefactually shrunk due to histological processing (Fig. 7**e**-**o**). Higher power examination of such images clearly showed the pericellular localisation of perlecan at the lacunar margins (Fig. 8**a**) and indicated the presence of small intracellular perlecan positive foci that were closely associated with the cell nucleus (Fig. 8**e**). These features were consistently noted in Z-stacks taken through other chondrons of the disc (Fig. 9). Detailed examination of selected image planes (*e.g.* Fig. 9**h**,**k**,**l**), showed the presence of punctate foci of perlecan fluorescence within the lacunar space and in intimate association with the cell nucleus (shown in detail in Fig. 10**a**-**c**). In the chondron shown in Fig. 10, Nomarski DIC observation of the blebbing cell membrane indicated that the punctate labelling pattern was intracellular (Fig. 10**d**-**f**).

In order to delineate the 3D-spatial organisation of perlecan within the disc chondrons, selected confocal Z-stacks were reconstructed as maximum intensity and surface-coded 3D models. Examination of the 3D reconstructed models *in silico* confirmed the 2D-spatial information identified from the stack views, showing interstitial, pericellular, and punctate intracellular labelling patterns (Fig. 11**a**-**c**). The intimate association of perlecan label with the cell nucleus was striking in the 3D projection views (Fig. 11); however, the punctate labelling pattern was less distinct than that observed in the 2D-optical sections due to interference from overlying structures in the focal plane (Fig. 11**c**).

Dual-confocal immunolocalisation of type VI collagen and perlecan established the close inter-relationship between these components in relation to the cells within the chondron structure (Fig. 12**a**,**d**). Type VI collagen and perlecan were co-distributed in the chondron and co-localised pericellularly, as demonstrated in 3D-overlay models, (Fig. 12**b**). Rendering the green fluorescence channel semi-transparent revealed the overlapping distributions of type VI collagen and perlecan around the cells (Fig. 12**c**) and showed that type VI collagen extended a greater distance from the cell into the inter-territorial ECM. Closer examination of the 3D-surface-rendered models revealed what appeared to be budding protrusions of perlecan, believed to represent vesicular deposits destined for matrix secretion.

Videos of sequential perlecan immunolocalisations through the full cell depth are also shown for the string of AF cells and single NP cell, depicted in Fig. 2. Supplementary videos 1 and 2 are available from the paper website. These videos clearly show the spatial distributions of perlecan in the specimens.

Discussion

The concept of the chondron as a structural functional entity in articular cartilage and IVD

The chondron concept was first introduced by Benninghoff (Benninghoff, 1925) who used polarised

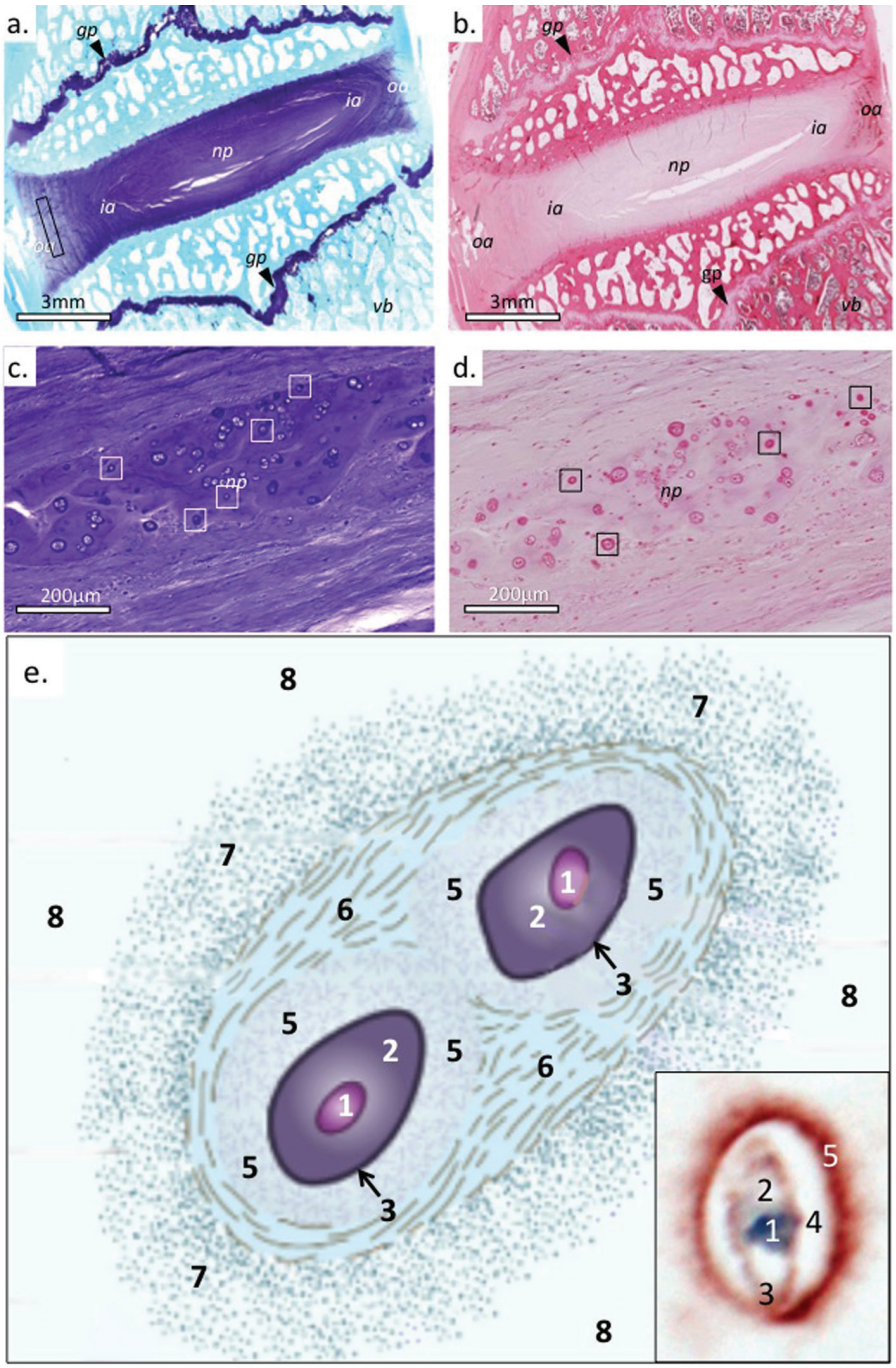

Fig. 1. **Histology of ovine IVD**. Vertical sections of ovine IVD stained with toluidine blue-fast green (**a**,**c**) and haematoxylin and eosin (**b**,**d**) showing the composite disc tissues. Boxed areas indicate representative ROI within the outer annulus (*oa*) and nucleus pulposus (*np*). *ia*, inner annulus; *gp*, growth plate; *vb*, vertebral body. (**e**) Schematic representation showing the structural features of a chondron based on observations made by Poole CA (1997-2008) and using terminology proposed by Pritzker and Aigner (2010) Inset shows immunolocalisation of pericellular perlecan. Image (**e**) reproduced from Gahunia and Pritzker (2020) with permission from Springer-Nature Publishers under licence number 4936150221393. 1, cell nucleus of chondrocyte; 2, chondrocyte cytoplasm; 3, chondrocyte plasma membrane; 4, lacuna space; 5, pericellular matrix; 6, fibrous pericellular capsule; 7, territorial matrix; 8, wider inter-territorial ECM.

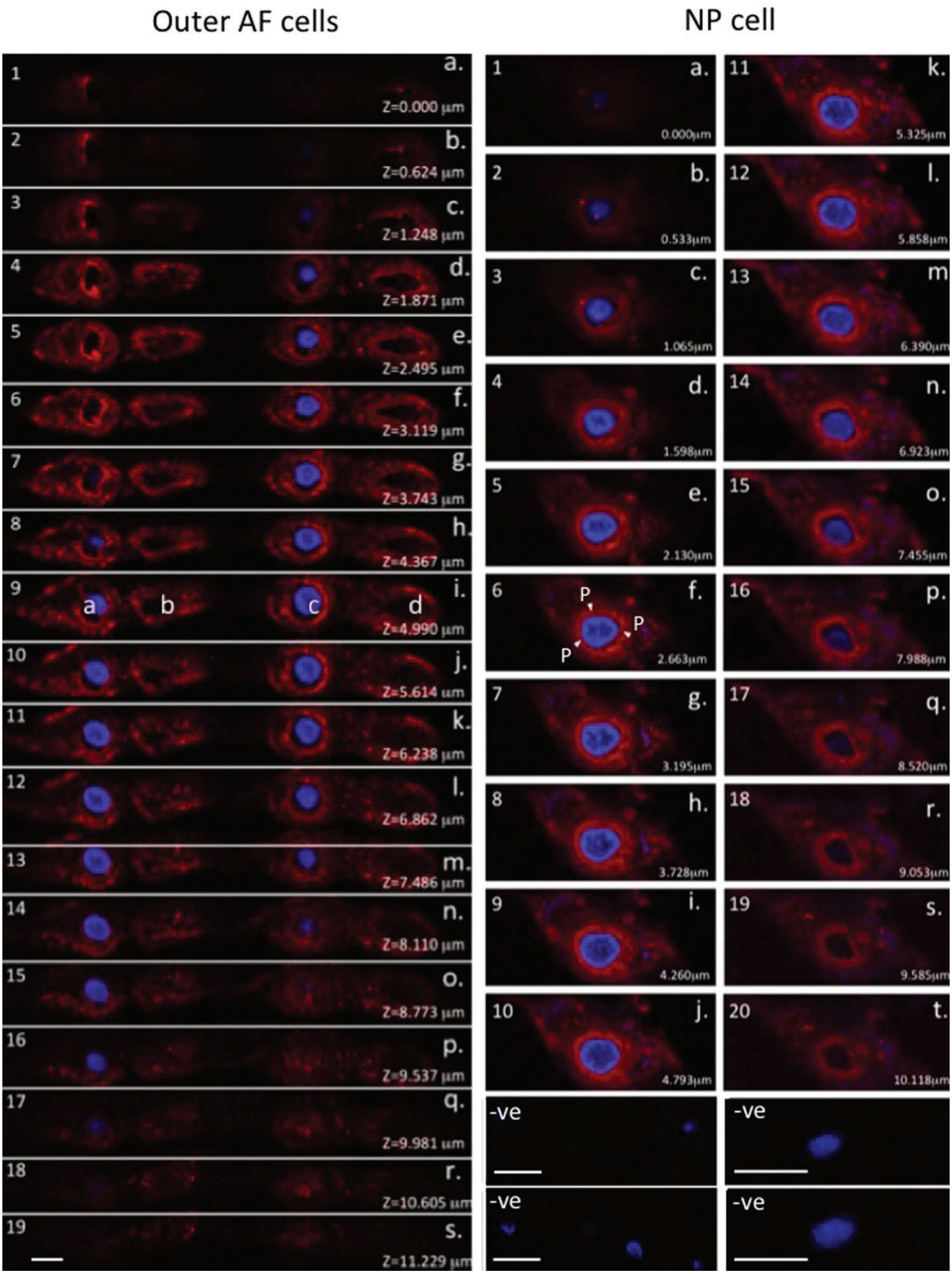

Fig. 2. Perlecan location in AF and NP cells. Composite image depicting perlecan immunofluorescence (red) in sequential optical sections of confocal Z-stacks through chondrons of the AF (left panel; **a-s**; sections # 1-19) and NP (right panel; **a-t**; sections # 1-20) of ovine IVD. Nuclear counterstaining in blue. The optical sections have been sampled at 0.6 µm increments through the full depth of the tissue section (Z position shown at bottom right of each image). The AF cell labelled **c** in section # 9 (i) is shown at higher magnification in Fig. 3 and followed from section # 7 through to # 10. Similarly, the NP cell shown is depicted at higher magnification in Fig. 4. Perlecan has a prominent pericellular distribution (P) with punctate foci identifiable within the lacunar space (refer to Fig. 3). Negative controls (bottom right panels) taken at low and high power indicate no non-specific labelling for perlecan. Scale bars 25 µm. Sequential images of the AF and NP cells are also provided as videos in supplementary videos 1 and 2.

light microscopy to demonstrate that the chondrocyte was surrounded by a specialised structure which he termed the *chondrone*. Interest in the chondron waned until 1969 (Szirmai, 1969) and 1974 (Szirmai, 1974) when interest was rekindled in this structure. More recently, Poole *et al*. published an extensive series of publications on cartilage chondrons (McGlashan *et al*., 2008; Poole, 1990a; Poole, 1993; Poole, 1997; Poole *et al*., 1984; Poole *et al*., 1985a; Poole *et al*., 1985b; Poole *et al*., 1987; Poole *et al*., 1988a; Poole *et al*., 1988b; Poole *et al*., 1988c; Poole *et al*., 1990b; Poole *et al*., 1991a; Poole *et al*., 1991b;). In 2010, Pritzker and Aigner proposed some definitions for the features evident in a chondron (Pritzker and Aigner, 2010). The Pritzker and Aigner terminology was adopted in the present study and an explanatory figure is provided to indicate the chondron's major structural features using this terminology (Fig. 1**e**). The 3D features of chondrons in the IVD have also been described (Cao *et al*., 2007) and variation in chondron morphology measured using confocal microscopy immunolocalisation of type VI collagen, which conveniently delineates the extent of the chondron structure (Youn *et al*., 2006). Perlecan also colocalises with type VI collagen in the chondron (Hayes *et al*., 2016) and has biomechanical properties (Wilusz *et al*., 2012) and, as shown in the present study, is localised in the PCM surrounding the disc cell within the chondron. Perlecan is a multifunctional PCM and ECM PG, where it stabilises these tissue compartments through its interactive properties with other matrix components. Perlecan also sequesters a number of growth factors, stimulates chondrogenesis and controls the proliferation and differentiation of chondrocytes and disc cells (Farach-Carson and Carson, 2007; Gomes *et al*., 2004; Knox *et al*., 2006; Lord *et al*., 2014; Melrose *et al*., 2006; Melrose *et al*., 2008a; Melrose, 2020). Perlecan also colocalises with elastin in

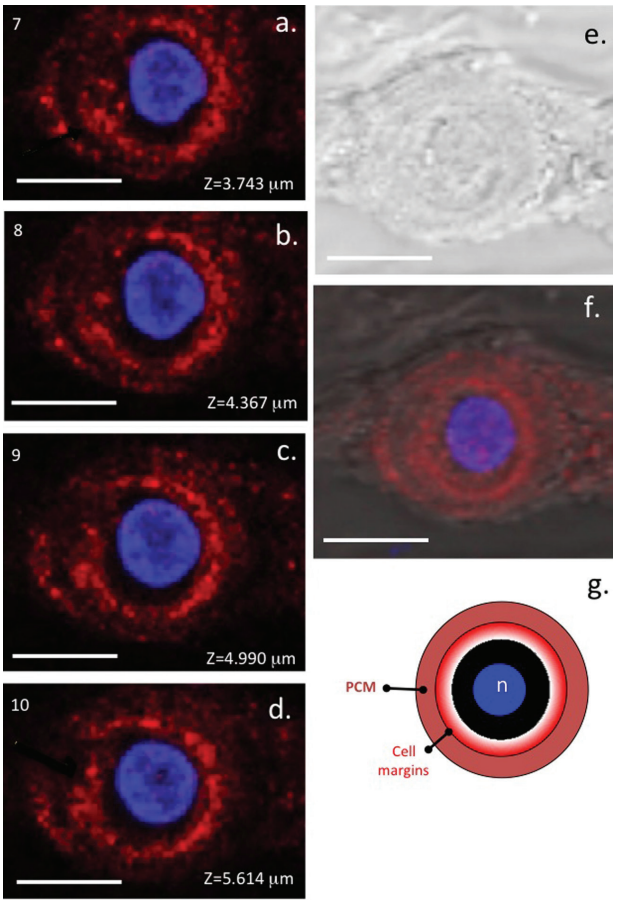

Fig. 3. Selected confocal optical sections through AF. (**a-d**) Selected confocal optical sections (# 7, 8, 9, 10) through an AF chondron immunolabelled for perlecan (red). Z position shown at bottom right of each image. Note prominent labelling of perlecan in pericellular matrix with bright foci at cell margins and adjacent to the nucleus. Nuclear counterstaining in blue. (**e**) Transmitted light image of chondron obtained by Normaski DIC optics. (**f**) Fluoresence/ DIC overlay image. (**g**) Schematic showing chondron structure. n, nucleus; PCM, pericellular matrix. Scale bars 25 µm.

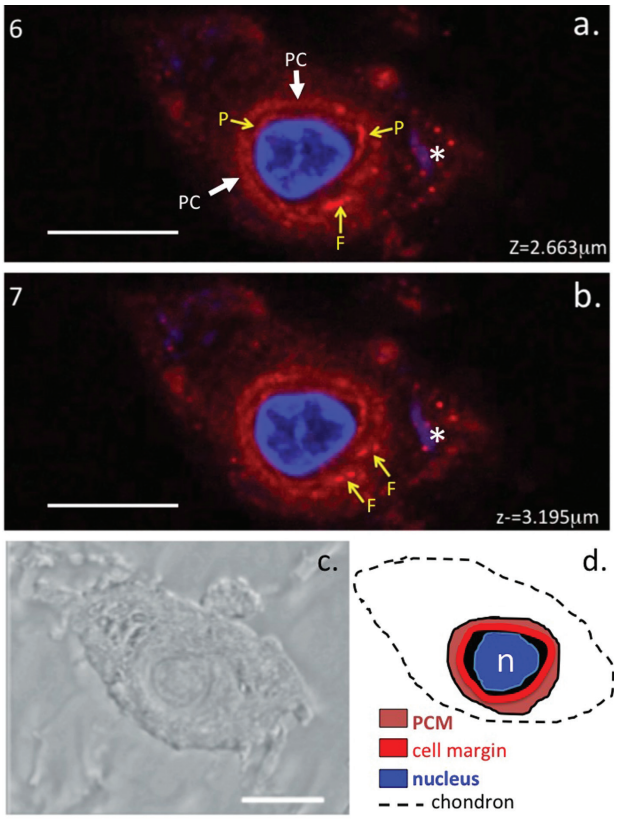

Fig. 4. Selected confocal optical sections through NP. (**a**,**b**) Selected confocal optical sections (# 6, # 7 of Fig. 2, right panel) through an NP chondron immunolabelled for perlecan (red). Z position shown at bottom right of each image. Cell nuclei counterstained blue. PC, denotes position of pericellular capsule (white arrows). Note also pericellular perlecan (P) and foci deposits (F) labelled with yellow arrows while asterisks indicate more removed foci. (**c**) Transmitted light image of chondron obtained by Normaski DIC optics. (**d**) Schematic showing chondron structure. n, nucleus; PCM, pericellular matrix. Scale bars 25 µm.

vascularised tissues and has roles in the coacervation of tropoelastin at the surface of AF cells, thereby contributing to assembly of fibrillin and elastin in elastic microfibrils (Hayes *et al.*, 2011a; Hayes *et al.*, 2011b; Hayes *et al.*, 2013; Hayes *et al.*, 2014). Perlecan also has interactive properties with type VI collagen in the chondron and also in translamellar cross-bridge structures that serve as internal stabilising struts between non-adjacent annular lamellae and also contain fibrillin-1, elastin and perlecan (Hayes *et al.*, 2016; Melrose *et al.*, 2008b; Yu *et al.*, 2015). The PCM is a strategic interface that links the disc cell with the adjacent extracellular micro-environment, and facilitates mechano-transductive responses by the disc cell that regulate disc tissue composition and function. Such interactions are therefore important in the maintenance of normal disc tissue homeostasis. Perlecan also has cytoprotective properties, protecting the disc cell from its harsh biomechanical microenvironment and conditions of low pH, oxygen tension and nutrition (Wilusz *et al.*, 2012; Wilusz *et al.*, 2014). Videos prepared to depict the sequential immunolocalisations of perlecan through the full depth of AF and NP cells enclosed in their chondrons provide complimentary visual information to the confocal perlecan immunolocalisations provided elsewhere in this study (see supplementary videos 1 and 2 on the paper website).

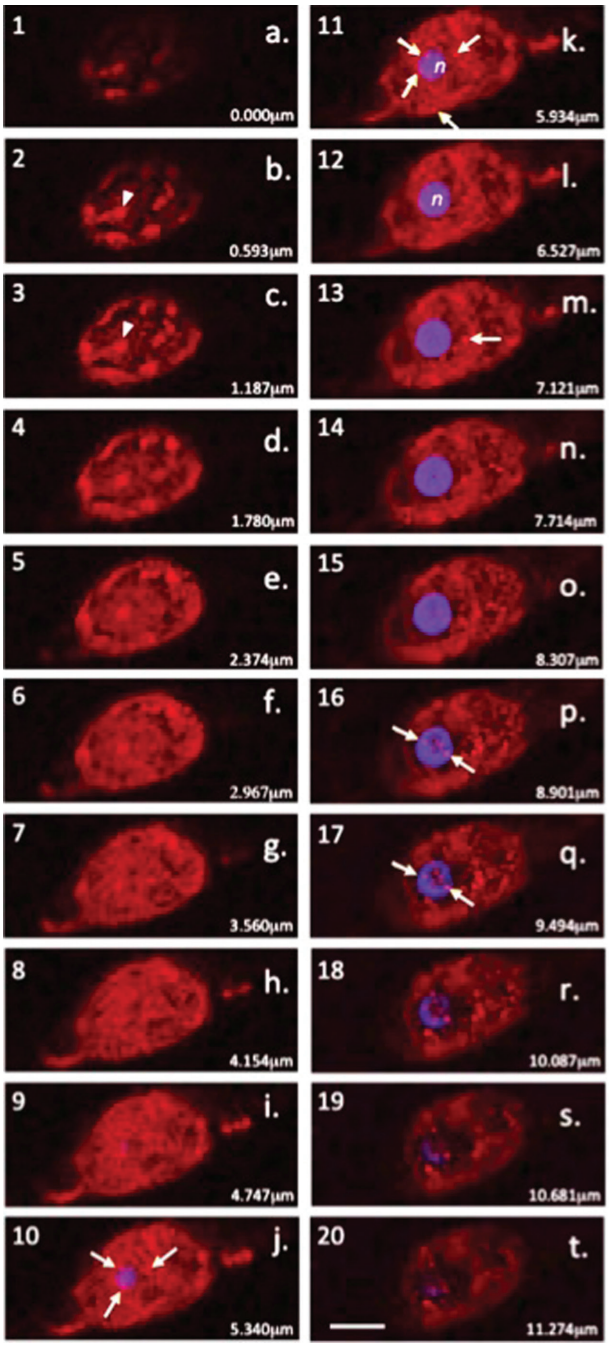

Fig. 5. Perlecan immunofluorescence in NP chondron. (**a-t**) Composite image depicting perlecan immunofluorescence (red) in sequential optical sections of confocal Z-stack through a NP chondron (sections # 1-20). Z position shown at bottom right of each image. Nuclear counterstaining in blue. White arrowheads highlight position of large perlecan-positive structures within chondron. White arrows denote punctate perlecan immunolabel closely associated with the cell nucleus. Sections # 3, 11 and 16 (**c**, **k**, **p**) are presented at higher magnification in Fig. 6. Scale bars 25 µm.

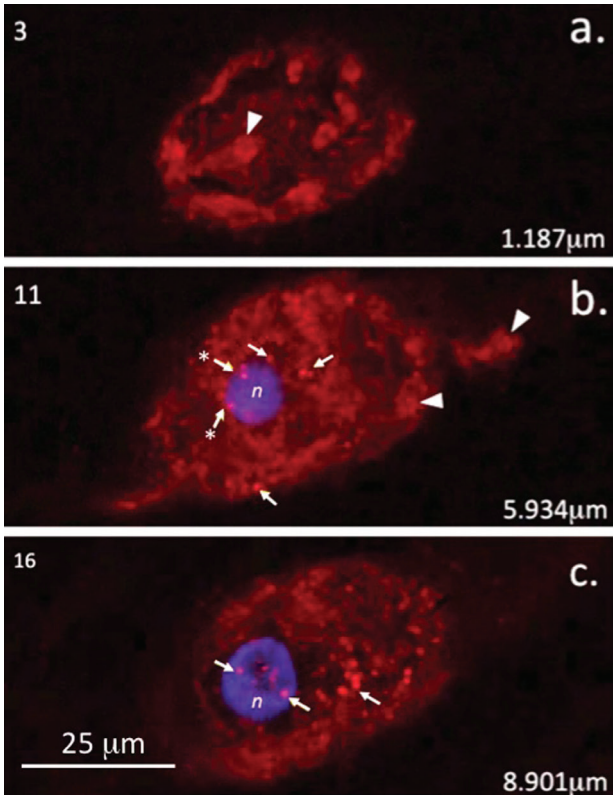

Fig. 6. Selected high magnification images of perlecan immunofluorescence in an NP chondron. (**a-c**) Selected confocal optical sections (Fig. 5**c**,**k**,**p**) taken through a NP chondron immunolabelled for perlecan (red)**.** Z position shown at bottom right of each image. Cell nuclei counterstained blue. (**c**) Presence of large perlecan-positive structures (white arrowheads) visible in superficial plane through chondron (section # 3). (**b**,**c**) Punctate perlecan immunolabel (white arrows) intimately associated with the cell nucleus and its margins (asterisks) (section # 11 and 16). Scale bars 25 µm.

Perlecan has previously been shown to be a pericellular component of AF and NP cells and has roles in the development of the IVD through its ability to undergo cell signalling with FGF-2, FGF-18 and FGFR-3 (Melrose *et al.*, 2003). Perlecan also interacts with type VI collagen and type XI collagen and has roles in the stabilisation of the disc cell PCM. Perlecan has not previously been shown to be an intracellular PG and may have previously unidentified roles to play in disc cell regulation through effects on nucleosomal organisation and transcription factor regulation. The current studies demonstrated a vesicular labelling pattern of perlecan within cells of both the NP and AF of the disc, with foci of perlecan immunolabel occurring in close association with the cell nucleus. A similar punctate labelling pattern of perlecan was also noted in the capsular matrix surrounding the disc cells. Although further work is required to substantiate these observations, the labelling patterns suggest that perlecan may be trafficked, by transport vesicles, between the cell nucleus and extracellular environment where it has established roles in disc cell regulation.

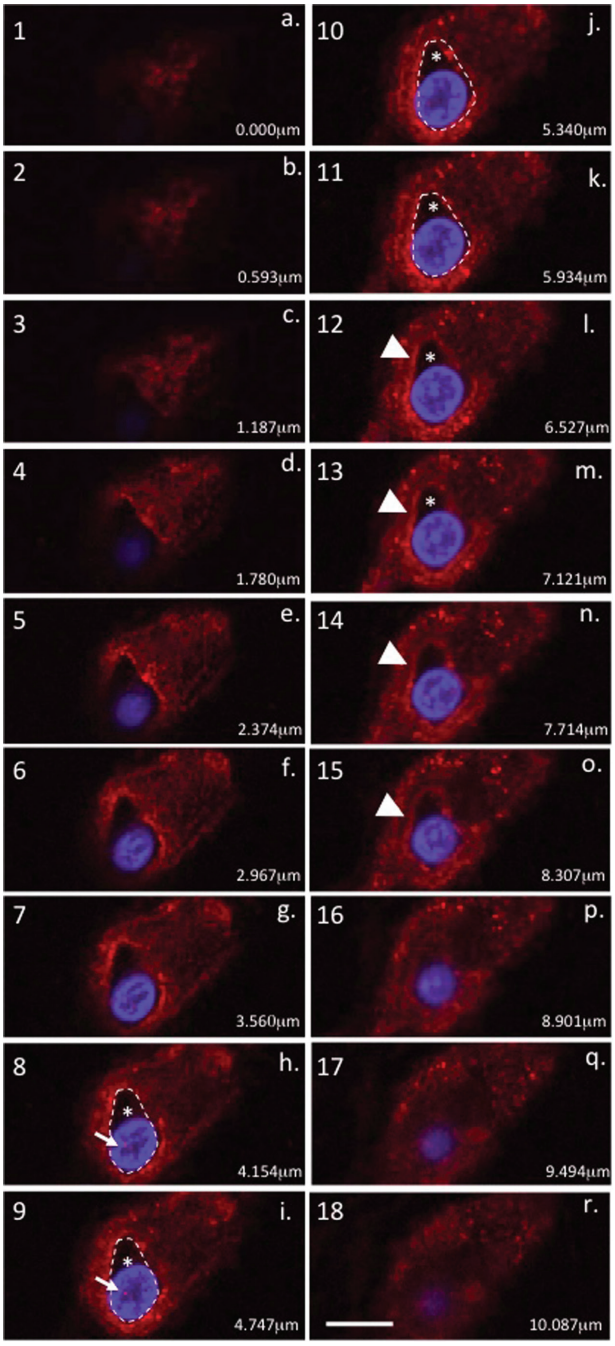

Fig. 7. Perlecan immunofluorescence in NP chondron. (**a**-**r**) Composite image depicting perlecan immunofluorescence (red) in sequential optical sections of confocal Z-stack through a NP chondron (sections # 1-18). Z position shown at bottom right of each image. Nuclear counterstaining in blue. (**h**-**m**) Lacuna space denoted by asterisk in sections # 8-13; margins of the lacuna indicated with dotted lines. (**h**,**i**) White arrows (sections # 8-9) indicate punctate perlecan label associated with the cell nucleus. (**l**-**o**) white arrowheads (sections # 12-15) highlight position of pericellular perlecan within chondron capsule. **h** and **l** are shown in detail in Fig. 8. Scale bars 25 µm.

Nuclear HS-proteoglycans

ECM HS-PGs have been observed to be shuttled to the nucleus in many cell types (Kovalszky *et al.*,

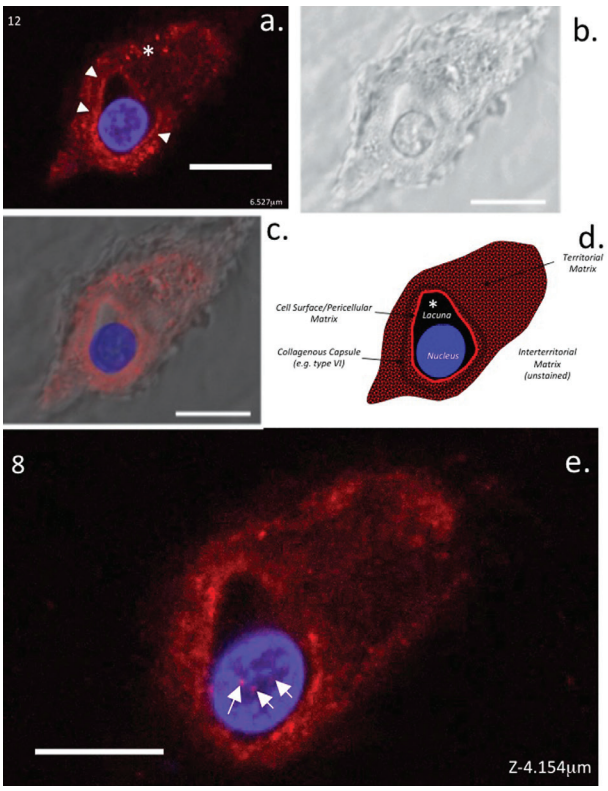

Fig. 8. Selected high magnification images of perlecan immunofluorescence in an NP chondron. (**a**) Detail of Fig. 7**l**, showing perlecan immunolocalisation (red) within a chondron of the NP. Nuclear counterstaining in blue. Z position shown at bottom right of image. White arrowheads indicate position of pericellular perlecan within chondron capsule. (**b**) Transmitted light (DIC) image. (**c**) Fluorescence/DIC overlay image. (**d**) Schematic showing zonal structure of chondron. (**e**) Detail of Fig. 7**h,** showing perlecan-positive foci within the cell nucleus (white arrows). Scale bars 25 µm.

2014; Ricard-Blum and Gondelaud, 2016; Stewart and Sanderson, 2014). GPC has been identified in the nucleus of neurons and glioma cells (Liang *et al.*, 1997), SDC-4 in the nucleus of cardiomyocytes, SDC-1 in fibrosarcoma cells and SDC-2 to the nucleus of tumour cells in osteochondromas (Schrage *et al.*, 2009). Increased expression of *Snail*, a repressor transcription factor, correlates with translocation of SDC-1 to the nucleus in prostate cancer cell lines (Farfán N *et al.*, 2020). The function of nuclear SDC-1 is unclear; however, it has been proposed to inhibit histone acetyltransferase and lead to chromatin compaction (Purushothaman *et al.*, 2011), decreasing DNA accessibility to transcription factors, effecting cell cycle control, decreased proliferation and the regulation of transcriptional machinery and protein transport to the nucleus (Kovalszky *et al.*, 2014).

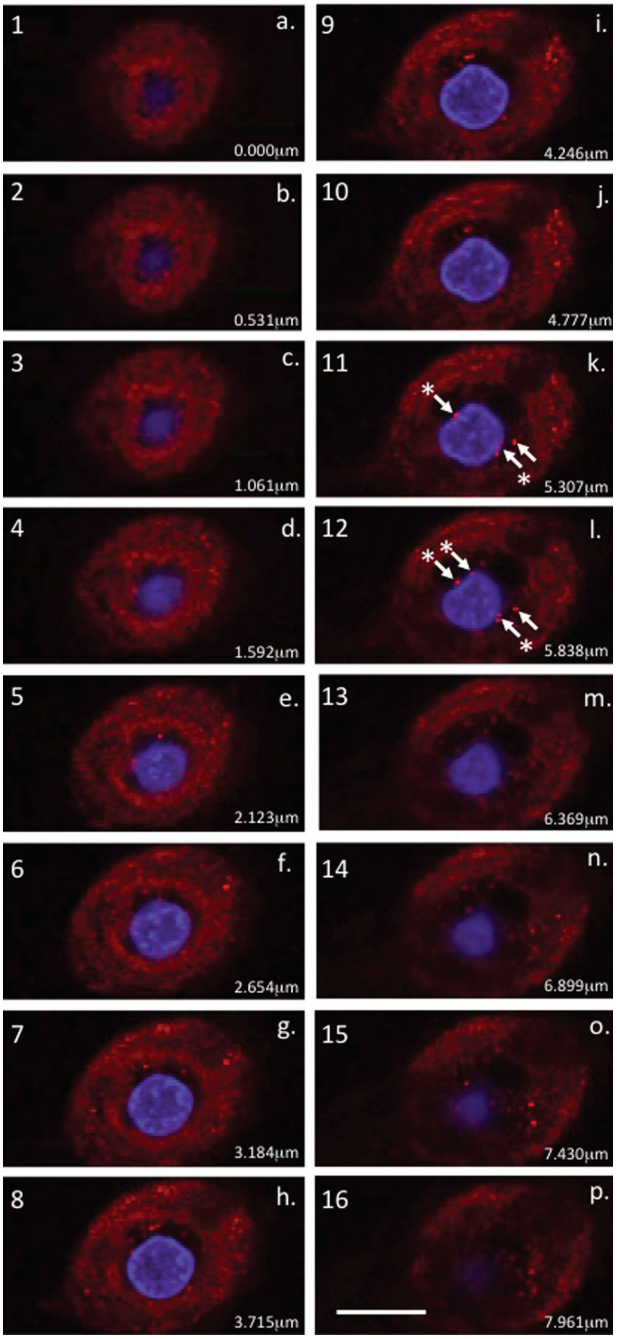

Fig. 9. Perlecan immunofluorescence in NP chondron. (**a-p**) Composite image depicting perlecan immunofluorescence (red) in sequential optical sections of confocal Z-stack through a NP chondron (sections # 1-16). Nuclear counterstaining in blue. Z position shown at bottom right of each image. White arrows with asterisks indicate perlecan-positive foci at nuclear margins, single arrows depict foci further removed from the nucleus. Selected images from this composite are depicted in detail in Fig. 10. Scale bars 25 µm.

Biosynthesis of proteoglycans

PG biosynthesis involves the synthesis of a protein core in the rough endoplasmic reticulum, followed by post-transitional addition of GAG in the smooth membrane systems (Geetha-Habib *et al.*, 1984; Ratcliffe *et al.*, 1985) of the Golgi complex (Kimura *et al.*, 1984). The PG is then exported to the extracellular environment in vesicles. The perinuclear (Golgi) region of chondrocytes is the major site of radio-sulphate incorporation (Godman and Lane, 1964; Kimata *et al.*, 1971) and of proteoglycan and GAG localisation (Pacifici *et al.*, 1983; Ratcliffe *et al.*, 1985; Song *et al.*, 2020; Vertel and Dorfman, 1978; Vertel and Dorfman, 1979; Vertel and Barkman, 1984). Addition of xylose to the core protein linkage region is a late endoplasmic reticulum or early Golgi event (Lohmander *et al.*, 1986) and step-wise addition of 2

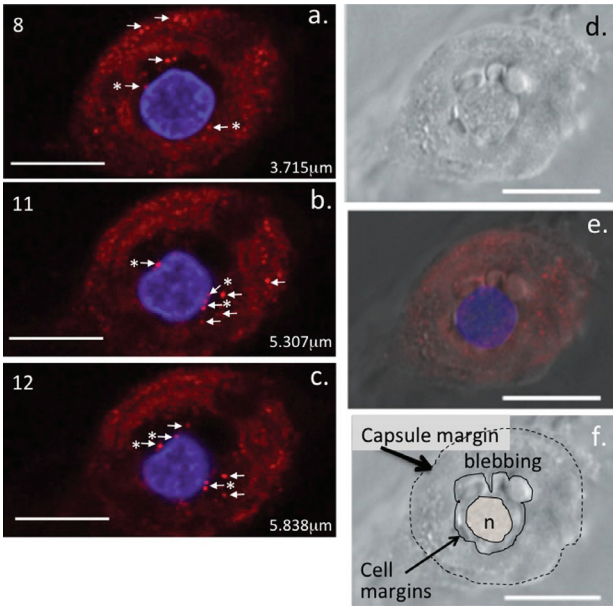

Fig. 10. Selected high magnification images of perlecan immunofluorescence in an NP chondron. (**a**,**b**,**c**) Selected sections from Fig. 9 showing punctate labelling of perlecan (red) within a chondron of the NP. White arrows indicate perlecan-positive foci within the chondron capsule, in the nuclear margins (asterisks). Nuclear counterstaining in blue. Z position shown at bottom right of each image. (**d**) Transmitted light DIC image of chondron (**e**) Fluorescence/DIC overlay image (**f**) Schematic illustrating position of cell nucleus (n) depicting cell margin, denoted by blebbing cell membrane (solid line), and margin of capsular matrix (dashed line). Scale bars 25 µm.

galactose residues then occurs followed by a GlcA residue to complete the Xyl-Gal-Gal-GlcA linkage region. The Xyl-Gal-Gal-GlcA tetrasaccharide linkage region acts as an acceptor molecule for the subsequent assembly of HS, CS and DS GAG chains through the co-ordinated and sequential action of a number of sulpho- and glycosyl transferase and synthase enzyme systems (Ethen *et al.*, 2015; Sasarman *et al.*, 2016). The vesicular perinuclear localisation of perlecan that was observed in the present study may thus represent endogenously-produced perlecan destined for secretion from the cytoplasmic compartment into the pericellular matrix environment of the chondron. The intranuclear localisation of perlecan-positive vesicles identified in confocal Z-stacks suggested a potentially novel role for this multifunctional PG.

FGF-1 and FGF-2 in the nucleus

FGF-2 is a member of the large FGF family of growth factors that bind heparin and HS and have modulatory effects on a wide range of cell types. FGF-2 stimulation of endothelial cells induces normal wound healing and tissue development through new blood vessel development in healthy tissues; however, it can also promote pathogenic conditions such as cancer and atherosclerosis. Growth factors translocated from the cell surface, such as FGF-2, can be imported into the nucleus and have direct biological roles regulated by nuclear HS-PGs (Levine and Prystowsky, 1995). FGFRs can also enter the nucleus during the cellular transition between proliferation and differentiation. Once nuclear, FGFRs may interact with chromatin remodelling proteins which alter the epigenetic state and transcriptional status of target genes (Tuzon *et al.*, 2019).

Nuclear heparan sulphate proteoglycans

The presence of nuclear HS-PGs has been demonstrated by many studies over the last 5 decades (Fedarko *et al.*, 1989; Hsia *et al.*, 2003; Ishihara and Conrad, 1989; Ishihara *et al.*, 1986) and correlated with cell proliferation (Fedarko *et al.*, 1989). Nuclear HS-PGs also have shuttling properties for protein kinase C-dependent nuclear localisation of FGF-2, shown to occur following corneal trauma (Hsia *et al.*, 2003). FGF-2 is also an extracellular mechano-transductive chondro-protective effector molecule in cartilage (Vincent and Saklatvala, 2006; Vincent *et al.*, 2007). Nuclear HS-PGs inhibit DNA topoisomerase I activity, which has important roles to play in the removal of DNA supercoils during transcription and DNA replication; in the re-annealing of DNA strands following strand breakage during re-combination and chromosomal condensation; and in the disentanglement of intertwined DNA strands during mitosis (Champoux, 2001; Wang, 2002). HS charge-mediated interactions represent a potential means whereby chromatin structure, nucleosomal function and thus gene expression are regulated (Buczek-Thomas *et al.*, 2008).

Regulation of intervertebral disc homeostasis by the Wnt signalling pathway

In humans, 19 Wnt protein family members act as morphogens establishing long-range concentration gradients that facilitate differential effects on cells depending on the cells location within the Wnt gradient (Rao and Kühl, 2010). Wnt proteins bind to perlecan domain II, which transport the Wnts in tissues and aids in the establishment of Wnt concentration gradients (Matsuo and Kimura-Yoshida, 2014). This is an important role for perlecan in tissue morphogenesis, Wnt family members are palmitoylated signalling glycoproteins with relatively poor solubility; however, these lipid-modified proteins bind with high affinity to perlecan domain II which maintains their solubility and allows perlecan to act as a Wnt transporter PG (Willert and Nusse, 2012). β-catenin is a key mediator of Wnt signalling (Willert and Nusse, 1998), perlecan

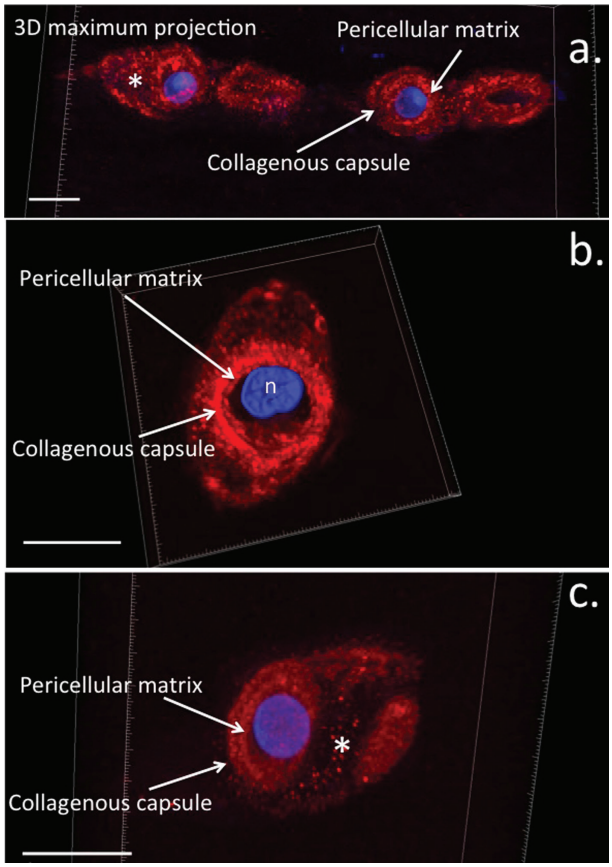

Fig. 11. 3D rendered image stack of AF chondron showing perlecan immunolocalisation. (**a**) 3D rendered image stack showing perlecan immunolocalisation (red) associated with a string of outer AF chondrons. Nuclear counterstaining in blue. 3D volume indicated by white boundary box. Note intimate association of perlecan with the cell nuclei (**b**,**c**) in 3D reconstructions of NP chondrons. The pericellular matrix and collagenous capsule of the chondron are highlighted. Asterisk denotes punctate labelling of perlecan associated with chondron. *N.B.* punctate labelling associated with cell nucleus is less conspicuous due to overlying structures. Scale bars 25 μm.

regulates Wnt signalling in *Drosophila* (Kamimura *et al.*, 2013; Lindner *et al.*, 2007) and humans (Lord *et al.*, 2014). The Wnt pathway is an important regulatory pathway in the IVD with key roles in IVD cell differentiation, morphogenesis, tissue remodelling/repair, and the control of IVD homeostasis (Clevers *et al.*, 2014; Kahn, 2014; Logan and Nusse, 2004). Wnt signalling is activated in IVD degeneration (Wang *et al.*, 2012) contributing to decreases in ECM production, senescence, and apoptosis of NP cells (Cully *et al.*, 2013; Hiyama *et al.*, 2010; Roberts *et al.*, 2006). Wnt-β catenin signalling is implicated in the increased degradation of IVD components *in vivo* through an elevation in the levels of MMP-1, MMP-2, and MMP-9 activity (Hiyama *et al.*, 2013; Hoyland *et al.*, 2008) and in fibrotic IVD changes mediated through interactions with TGF-β (Lord *et al.*, 2018; Piersma *et al.*, 2015; Sun *et al.*, 2015; Zhou *et al.*, 2012).

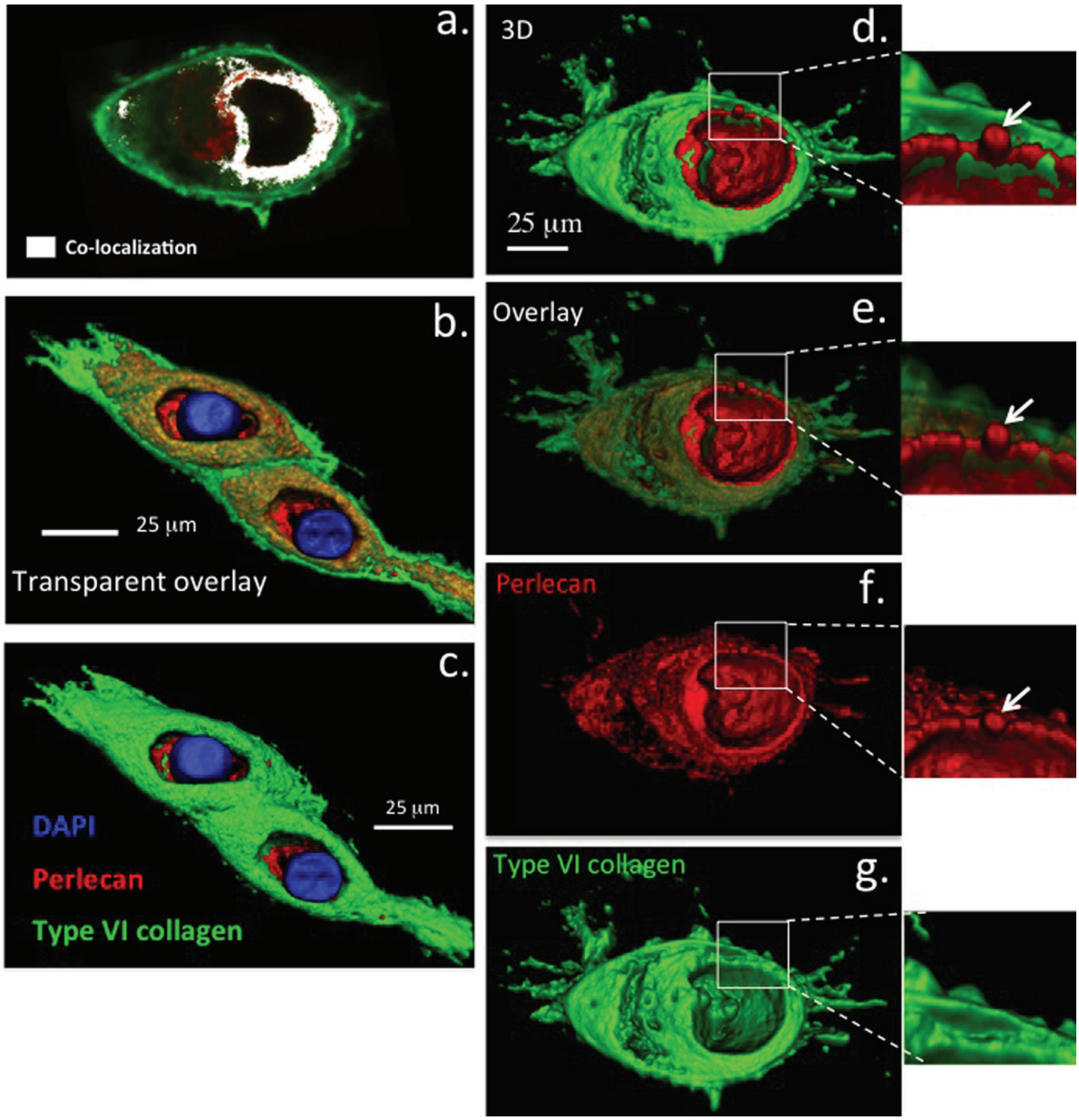

Fig. 12. PCM organisation in NP chondron cells. (**a**, **d-g**) Matrix organisation of disc chondrons from the NP. (**b**,**c**) AF dual labelled for perlecan (red) and type VI collagen (green). Cell nuclei shown in blue. (**a**) Colocalisation of type VI collagen and perlecan within the pericellular matrix of a NP chondron denoted by white overlay mask. (**b-g**) Surface-rendered 3D reconstructions, showing the organisation of perlecan and type VI collagen within disc chondrons. (**b** and **e**) The type VI collagen labelling pattern (green) has been rendered semi-transparent to show details of the underlying perlecan organisation (orange-red). (**d**) the cell contents have been lost from the lacuna during histological processing. Pericellular perlecan, lining the unoccupied lacuna, can be seen intimately associated with the type VI collagen within the capsular matrix. (**d-g)** boxed ROIs show detail of budding perlecan protrusions at the innermost surface of the chondron capsule, *i.e.* adjacent to the plasma membrane. Fig. modified from (Hayes and Melrose, 2019) under the terms of the CC-BY-SA license. Copyright 2016, The Authors.

Nuclear heparanase

Nuclear heparanase, as part of an active chromatin complex, regulates mitotic spindle formation and maintains chromosome stability (Yang *et al.*, 2018). Heparanase degrades nuclear SDC-1 and enhances histone acetyl transferase aiding genes which aggressively promote tumour progression.

The regulatory roles of HIF-1α in the nucleus of NP and AF cells

HIF-1α is a key transcriptional factor in the IVD that is activated by hypoxia and may also be essential for the regulation of nuclear heparanase activity (He *et al.*, 2004). Blocking the NF-κB signal transduction pathway also decreases heparanase mRNA expression *in vitro* (Andela *et al.*, 2000), thus NF-κB may also regulate heparanase *in vivo*. Degradation of nuclear SDC-1 by heparanase enhances histone acetyltransferase activity and promotes expression of genes that aggressively drive the attainment of a tumour phenotype (Purushothaman *et al.*, 2011). Prolyl-4-hydroxylase controls the transactivation of NF-κB/p65 (Li *et al.*, 2015) and enhances the catabolic effects of inflammatory cytokines on cells in the NP. Expression of the PHDs is selectively controlled by HIF-1 and HIF-2 in NP cells (Fujita *et al.*, 2012) thus HIF-1 and 2 also indirectly regulates NF-κB and heparanase activity, and also now potentially perlecan.

Regulation of pro-inflammatory cytokines by HIF-1α, MMPs and ADAMTS-4, 5 through SDC-4 and how it impacts on intervertebral disc degeneration

Pro-inflammatory cytokines, such as TNF-α and IL-1β, upregulate MMP and ADAMTS expression in the IVD and, when activated, these result in IVD degeneration and failure of the functional biomechanical properties of the IVD (Roughley, 2004). During IVD degeneration, increased ADAMTS-4 and ADAMTS-5 activity results in an imbalance in anabolic and catabolic events in the IVD and cleavage and clearance of aggrecan results in impaired biomechanical competence in the degenerate IVD (Wang *et al.*, 2011). Inflammatory cytokines such as TNF-α and IL-1β result in an upregulation of SDC-4 synthesis in NP cells (Fears and Woods, 2006). SDC-4 selectively interacts with pro-ADAMTS-5 at the cell surface promoting its activation and aggrecan degradation (Mwale, 2014; Wang *et al.*, 2011). SDC-4 and ADAMTS-5-generated aggrecan neoepitope levels show a strong correlation with aggrecan depletion in the IVD and with IL-1β and TNF-α levels showing the interdependence of all of these components in IVD degeneration (Binch *et al.*, 2016). The PHD-HIF-1 axis controls expression of SDC-4 in NP cells (Fujita *et al.*, 2014). Thus HIF-1α not only provides cell survival properties to the IVD but it also regulates disc degeneration.

Conclusions

As far as is known, this is the first study to immunolocalise perlecan intracellularly within IVD cells and thus identify a potentially novel regulatory area for this multifunctional HS PG within the disc. Several perlecan ligands are also known to be nuclear and cytoplasmic components (*Wnt, FGF2, FGFR1*); however, it is not known if these interact with nuclear perlecan in the same way as they interact with perlecan in the PCM. Future experimental research on the IVD should examine this possibility and determine the physiological significance of such interactions. This may open up a new arena of cellular regulation and provide novel avenues for the treatment of disc degeneration and the alleviation of low back pain.

Acknowledgements

This study was funded by Melrose Personal Fund, Sydney, Australia.

Disclosures

The authors have no financial disclosures or conflicts to report.

References

Andela VB, Schwarz EM, Puzas JE, O'Keefe RJ, Rosier RN (2000) Tumor metastasis and the reciprocal regulation of prometastatic and antimetastatic factors by nuclear factor κB. Cancer Res **60**: 6557-6562.

Ayad S, Marriott A, Morgan K, Grant ME (1989). Bovine cartilage types VI and IX collagens. Characterization of their forms *in vivo*. Biochem J **262**: 753-761.

Benninghoff A (1925) Form und Bau der Gelenkknorpel in Ihren Bezeihungen zur Funktion. Zweiter Tiel. Der Aufbau des Gelenkknorpels in seinen Bezeihungen zur Funktion. Z Zellforsch **2**: 783-862.

Binch ALA, Shapiro IM, Risbud MV (2016) Syndecan-4 in intervertebral disc and cartilage: saint or synner? Matrix Biol **52-54**: 355-362.

Breitkreutz D, Koxholt I, Thiemann K, Nischt R (2013) Skin basement membrane: the foundation of epidermal integrity–BM functions and diverse roles of bridging molecules nidogen and perlecan. Biomed Res Int **2013**: 179784. DOI: 10.1155/2013/179784.

Buczek-Thomas JA, Hsia E, Rich CB, Foster JA, Nugent MA (2008) Inhibition of histone acetyltransferase by glycosaminoglycans. J Cell Biochem **105**: 108-120.

Cao L, Guilak F, Setton LA (2007) Three-dimensional morphology of the pericellular matrix of intervertebral disc cells in the rat. J Anat **211**: 444-452.

Champoux JJ (2001) DNA topoisomerases: structure, function, and mechanism. Annu Rev Biochem **70**: 369-413.

Clevers H, Loh, KM, Nusse, R (2014) An integral program for tissue renewal and regeneration: Wnt signaling and stem cell control. Science **346**: 1248012. DOI: 10.1126/science.1248012.

Cohen I, Grassel S, Murdoch AD, Iozzo RV (1993) Structural characterization of the complete human perlecan gene and its promoter. Proc Natl Acad Sci U S A **90**: 10404-10408.

Cully M (2013) Degenerative disc disease: altered Wnt signalling in intervertebral disc degeneration. Nat Rev Rheumatol **9**: 136. DOI: 10.1038/nrrheum.2013.22.

Ethen C, Machacek M, Prather B, Tatge T, Yu H, Wu ZL (2015) Nonradioactive glycosyltransferase and sulfotransferase assay to study glycosaminoglycan biosynthesis. Methods Mol Biol **1229**: 431-441.

Farach-Carson M, Carson DD (2007) Perlecan – a multifunctional extracellular proteoglycan scaffold. Glycobiology **17**: 891-905.

Farfán N, Orellana-Serradell O, Herrera D, Chrzanowsky D, Cubillos P, Marín G, De Herreros AAG, Castellón EA, Contreras HR (2020) SNAIL expression correlates with the translocation of syndecan 1 intracellular domain into the nucleus in prostate cancer cell lines. Int J Mol Med **45**: 1073-1080.

Fears CY, Woods A (2006) The role of syndecans in disease and wound healing. Matrix Biol **25**: 443-456.

Fedarko NS, Ishihara M, Conrad HE (1989) Control of cell division in hepatoma cells by exogenous heparan sulfate proteoglycan. J Cell Physiol **139**: 287-294.

Fujita N, Hirose Y, Tran CM, Chiba K, Miyamoto T, Toyama Y, Shapiro IM, Risbud MV (2014) HIF-1-PHD2 axis controls expression of syndecan 4 in nucleus pulposus cells. FASEB J **28**: 2455-2465.

Fujita N, Markova D, Anderson DG, Chiba K, Toyama Y, Shapiro IM, Risbud MV (2012) Expression of prolyl hydroxylases (PHDs) is selectively controlled by HIF-1 and HIF-2 proteins in nucleus pulposus cells of the intervertebral disc: distinct roles of PHD2 and PHD3 proteins in controlling HIF-1α activity in hypoxia. J Biol Chem **287**: 16975-16986.

Gahunia H, Pritzker KPH (2020) Structure and function of articular cartilage. In: Articular cartilage of the knee, health, disease and therapy (eds. Gahunia H, Gross A, Pritzker K, Babyn P, Murnaghan, L), Springer, New York. pp 3-70.

Geetha-Habib M, Campbell SC, Schwartz NB (1984) Subcellular localization of the synthesis and glycosylation of chondroitin sulfate proteoglycan core protein. J Biol Chem **259**: 7300-7310.

Godman G, Lane N (1964) On the site of sulfation in the chondrocyte. J Cell Biol **21**: 353-366.

Gomes RJ, Farach-Carson MC, Carson DD (2004) Perlecan functions in chondrogenesis: insights from *in vitro* and *in vivo* models. Cells Tissues Organs **176**: 79-86.

Hayes A, Gibson MA, Shu C, Melrose J (2014) Confocal microscopy demonstrates association of LTBP-2 in fibrillin-1 microfibrils and colocalisation with perlecan in the disc cell pericellular matrix. Tissue Cell **46**: 185-197.

Hayes A, Lord MS, Smith SM, Smith MM, Whitelock JM, Weiss AS, Melrose J (2011a) Colocalization *in vivo* and association *in vitro* of perlecan and elastin. Histochem Cell Biol **136**: 437-454.

Hayes A, Melrose J (2019) Glycosaminoglycan and proteoglycan biotherapeutics in articular cartilage protection and repair strategies: novel approaches to visco-supplementation in orthobiologics. Adv Therap **2**: 1900034. DOI: 10.1002/adtp.201900034.

Hayes A, Shu CC, Lord MS, Little CB, Whitelock JM, Melrose J (2016) Pericellular colocalisation and interactive properties of type VI collagen and perlecan in the intervertebral disc. Eur Cell Mater **32**: 40-57.

Hayes A, Smith SM, Gibson MA, Melrose J (2011b) Comparative immunolocalization of the elastin fiber-associated proteins fibrillin-1, LTBP-2, and MAGP-1 with components of the collagenous and proteoglycan matrix of the fetal human intervertebral disc. Spine (Phila Pa 1976) **36**: E1365-1372.

Hayes A, Smith SM, Melrose J (2013) Comparative immunolocalisation of fibrillin-1 and perlecan in the human foetal, and HS-deficient hspg2 exon 3 null mutant mouse intervertebral disc. Histochem Cell Biol **139**: 1-11.

He X, Brenchley PE, Jayson GC, Hampson L, Davies J, Hampson IN (2004) Hypoxia increases heparanase-dependent tumor cell invasion, which can be inhibited by antiheparanase antibodies. Cancer Res **64**: 3928-3933.

Hiyama A, Sakai D, Risbud MV, Tanaka M, Arai F, Abe K, Mochida J (2010) Enhancement of intervertebral disc cell senescence by WNT/β-catenin signaling-induced matrix metalloproteinase expression. Arthritis Rheum **62**: 3036-3047.

Hiyama A, Yokoyama K, Nukaga T, Sakai D, Mochida J (2013) A complex interaction between Wnt signaling and TNF-α in nucleus pulposus cells. Arthritis Res Ther **15**: R189. DOI: 10.1186/ar4379.

Hoyland J, Le Maitre C, Freemont AJ (2008) Investigation of the role of IL-1 and TNF in matrix degradation in the intervertebral disc. Rheumatology (Oxford) **47**: 809-814.

Hsia E, Richardson TP, Nugent MA (2003) Nuclear localization of basic fibroblast growth factor is mediated by heparan sulfate proteoglycans through protein kinase C signaling. J Cell Biochem **88**: 1214-1225.

Ishihara M, Conrad HE (1989) Correlations between heparan sulfate metabolism and hepatoma growth. J Cell Physiol **138**: 467-476.

Ishihara M, Fedarko NS, Conrad HE (1986) Transport of heparan sulfate into the nuclei of hepatocytes. J Biol Chem **261**: 13575-13580.

Kahn M (2014) Can we safely target the WNT pathway? Nat Rev Drug Discov **13**: 513-532.

Kamimura K, Ueno K, Nakagawa J, Hamada R, Saitoe M, Maeda N (2013) Perlecan regulates

bidirectional Wnt signaling at the *Drosophila* neuromuscular junction. J Cell Biol **200**: 219-233.

Kimata K, Okayama M, Suzuki S, Suzuki I, Hoshino M (1971) Nascent mucopolysaccharides attached to the Golgi membrane of chondrocytes. Biochim Biophys Acta **237**: 606-610.

Kimura J, Lohmander LS, Hascall VC (1984) Studies on the biosynthesis of cartilage proteoglycan in a model system of cultured chondrocytes from the Swarm rat chondrosarcoma. J Cell Biochem **26**: 261-278.

Kirn-Safran C, Farach-Carson MC, Carson DD (2009) Multifunctionality of extracellular and cell surface heparan sulfate proteoglycans. Cell Mol Life Sci **66**: 3421-3434.

Knox S, Whitelock JM (2006) Perlecan: how does one molecule do so many things? Cell Mol Life Sci **63**: 2435-2445.

Kovalszky I, Hjerpe A, Dobra K (2014) Nuclear translocation of heparan sulfate proteoglycans and their functional significance. Biochim Biophys Acta **1840**: 2491-2497.

Kvist AJ, Johnson AE, Morgelin M, Gustafsson E, Bengtsson E, Lindblom K, Aszodi A, Fassler R, Sasaki T, Timpl R, Aspberg A (2006). Chondroitin sulfate perlecan enhances collagen fibril formation. Implications for perlecan chondrodysplasias. J Biol Chem **281**: 33127-33139.

Leadbeater W, Gonzalez AM, Logaras N, Berry M, Turnbull JE, Logan A (2006) Intracellular trafficking in neurones and glia of fibroblast growth factor-2, fibroblast growth factor receptor 1 and heparan sulphate proteoglycans in the injured adult rat cerebral cortex. J Neurochem **96**: 1189-1200.

Levine JE, Prystowsky MB (1995) Polypeptide growth factors in the nucleus: a review of function and translocation. Neuroimmunomodulation **2**: 290-298.

Li J, Yuan W, Jiang S, Ye W, Yang H, Shapiro IM, Risbud MV (2015) Prolyl-4-hydroxylase domain protein 2 controls NF-κB/p65 transactivation and enhances the catabolic effects of inflammatory cytokines on cells of the nucleus pulposus. J Biol Chem **290**: 7195-7207.

Liang Y, Haring M, Roughley PJ, Margolis RK, Margolis RU (1997) Glypican and biglycan in the nuclei of neurons and glioma cells: presence of functional nuclear localization signals and dynamic changes in glypican during the cell cycle. J Cell Biol **139**: 851-864.

Lindner J, Hillman PR, Barrett AL, Jackson MC, Perry TL, Park Y, Datta S. (2007) The *Drosophila* Perlecan gene trol regulates multiple signaling pathways in different developmental contexts. BMC Dev Biol **7**: 121. DOI: 10.1186/1471-213X-7-121.

Logan C, Nusse R (2004) The Wnt signaling pathway in development and disease. Annu Rev Cell Dev Biol **20**: 781-810.

Lohmander L, Hascall VC, Yanagishita M, Kuettner KE, Kimura JH (1986) Post-translational events in proteoglycan synthesis: kinetics of synthesis of chondroitin sulfate and oligosaccharides on the core protein. Arch Biochem Biophys **250**: 211-227.

Lord M, Chuang CY, Melrose J, Davies MJ, Iozzo RV, Whitelock JM (2014) The role of vascular-derived perlecan in modulating cell adhesion, proliferation and growth factor signaling. Matrix Biol **35**: 112-122.

Lord M, Tang F, Rnjak-Kovacina J, Smith JGW, Melrose J, Whitelock JM (2018) The multifaceted roles of perlecan in fibrosis. Matrix Biol **68-69**: 150-166.

Matsuo I, Kimura-Yoshida C (2014) Extracellular distribution of diffusible growth factors controlled by heparan sulfate proteoglycans during mammalian embryogenesis. Philos Trans R Soc Lond B Biol Sci **369**: 20130545. DOI: 10.1098/rstb.2013.0545.

McGlashan S, Cluett EC, Jensen CG, Poole CA (2008) Primary cilia in osteoarthritic chondrocytes: from chondrons to clusters. Dev Dyn **237**: 2013-2020.

McLeod M, Wilusz RE, Guilak F (2013) Depth-dependent anisotropy of the micromechanical properties of the extracellular and pericellular matrices of articular cartilage evaluated via atomic force microscopy. J Biomech **46**: 586-592.

Melrose J (2020) Perlecan, a modular instructive proteoglycan with diverse functional properties. Int J Biochem Cell Biol **128**: 105849. DOI: 10.1016/j.biocel.2020.105849.

Melrose J, Hayes AJ, Whitelock JM, Little CB (2008a) Perlecan, the "jack of all trades" proteoglycan of cartilaginous weight-bearing connective tissues. Bioessays **30**: 457-469.

Melrose J, Roughley P, Knox S, Smith S, Lord M, Whitelock J (2006) The structure, location, and function of perlecan, a prominent pericellular proteoglycan of fetal, postnatal, and mature hyaline cartilages. J Biol Chem **281**: 36905-36914.

Melrose J, Smith S, Ghosh P, Whitelock J (2003) Perlecan, the multidomain heparan sulfate proteoglycan of basement membranes, is also a prominent component of the cartilaginous primordia in the developing human fetal spine. J Histochem Cytochem **51**: 1331-1341.

Melrose J, Smith SM, Appleyard RC, Little CB. (2008b) Aggrecan, versican and type VI collagen are components of annular translamellar crossbridges in the intervertebral disc. Eur Spine J **17**: 314-324.

Melrose J, Smith SM, Smith MM, Little CB. (2008c) The use of Histochoice for histological examination of articular and growth plate cartilages, intervertebral disc and meniscus. Biotech Histochem **83**: 47-53.

Murdoch AD, Dodge GR, Cohen I, Tuan RS, Iozzo RV (1992) Primary structure of the human heparan sulfate proteoglycan from basement membrane (HSPG2/perlecan). A chimeric molecule with multiple domains homologous to the low density lipoprotein receptor, laminin, neural cell adhesion molecules, and epidermal growth factor. J Biol Chem **267**: 8544-8557.

Mwale F (2014) Syndecan 4 signaling and intervertebral disc degeneration. Am J Pathol **184**: 2371-2373.

Nakamura K, Ikeuchi T, Nara K, Rhodes CS, Zhang P, Chiba Y, Kazuno S, Miura Y, Ago T, Arikawa-Hirasawa E, Mukouyama YS, Yamada Y (2019) Perlecan regulates pericyte dynamics in the maintenance and repair of the blood-brain barrier. J Cell Biol **218**: 3506-3525.

Noonan D, Fulle A, Valente P, Cai S, Horigan E, Sasaki M, Yamada Y, Hassell JR (1991) The complete sequence of perlecan, a basement membrane heparan sulfate proteoglycan, reveals extensive similarity with laminin A chain, low density lipoprotein-receptor, and the neural cell adhesion molecule. J Biol Chem **266**: 22939-22947.

Pacifici M, Soltesz R, Thal G, Shanley DJ, Boettiger D, Holtzer H (1983) Immunological characterization of the major chick cartilage proteoglycan and its intracellular localization in cultured chondroblasts: a comparison with Type II procollagen. J Cell Biol **97**: 1724-1736.

Piersma B, Bank RA, Boersema M (2015) Signaling in fibrosis: TGF-β, WNT, and YAP/TAZ converge. Front Med (Lausanne) **2**: 14. DOI: 10.3389/fmed.2015.00059.

Poole CA (1990a) Chondrons extracted from articular cartilage: methods and applications. In: Methods in cartilage research. (ed. Maroudas A, Kuettner KE), Academic Press, London, San Diego, pp 78-83.

Poole CA (1993) Structure and function of articular cartilage matrices. In: Cartilage Degradation: Basic and Clinical Aspects (ed. Woessner F, Howell D), Marcel Dekker: New York., New York, pp 1-35.

Poole CA (1997) Articular cartilage chondrons: form, function and failure. J Anat **191**: 1-13.

Poole CA, Ayad S, Schofield JR (1988a) Chondrons from articular cartilage. (IV). Immunolocalisation of type VI collagen in the pericellular capsule of isolated canine chondrons. J Cell Sci **90**: 635-645.

Poole CA, Flint MH, Beaumont BW (1984) Morphological and functional inter-relationships of articular cartilage matrices. J Anat **38**: 113-138.

Poole CA, Flint MH, Beaumont BW (1985a) Morphology of the pericellular capsule in articular cartilage revealed by hyaluronidase digestion. J Ultrastruct Res **91**: 13-23.

Poole CA, Flint MH, Beaumont BW (1985b) Analysis of the morphology and function of primary cilia in connective tissues: a cellular cybernetic probe? Cell Motil **5**: 175-193.

Poole CA, Flint MH, Beaumont BW (1987) Chondrons in cartilage: ultrastructural analysis of the pericellular microenvironment in adult human articular cartilages. J Orthop Res **5**: 509-522.

Poole CA, Flint MH, Beaumont BW (1988b) Chondrons extracted from canine tibial cartilage: preliminary report on their isolation and structure. J Orthop Res **6**: 408-441.

Poole CA, Glant TT, Schofield JR (1991a) Chondrons from articular cartilage. (IV). Immunolocalization of proteoglycan epitopes in isolated canine tibial chondrons. J Histochem Cytochem **39**: 1175-1187.

Poole CA, Honda T, Skinner SJM, Schofield JR, Hyde KF, Shinkai H (1990b) Chondrons from articular cartilage:(II) Analysis of the glycosaminoglycans in the cellular microenvironment of isolated canine chondrons. Conn Tiss Res **24**: 1-12.

Poole CA, Matsuoka A, Schofield JR (1991b) Chondrons from articular cartilage (III). Morphologic changes in the cellular microenvironment of chondrons isolated from osteoarthritic cartilage. Arthr Rheum **34**: 22-35.

Poole CA, Wotton SF, Duance VC (1988c) Localisation of type IX collagen in chondrons isolated from porcine articular cartilage and rat chondrosarcoma. Histochem J **20**: 567-574.

Pritzker K, Aigner T (2010) Terminology of osteoarthritis cartilage and bone histopathology – a proposal for a consensus. Osteoarthritis Cartilage **18**: S7-S9.

Purushothaman A, Hurst DR, Pisano C, Mizumoto S, Sugahara K, Sanderson RD (2011) Heparanase-mediated loss of nuclear syndecan-1 enhances histone acetyltransferase (HAT) activity to promote expression of genes that drive an aggressive tumor phenotype. J Biol Chem **286**: 30377-30383.

Rao T, Kühl M (2010) An updated overview on Wnt signaling pathways: a prelude for more. Circ Res **106**: 1798-1806.

Ratcliffe A, Fryer PR, Hardingham TE (1985) Proteoglycan biosynthesis in chondrocytes: protein A-gold localization of proteoglycan protein core and chondroitin sulfate within Golgi subcompartments. J Cell Biol **101**: 2355-2365.

Ricard-Blum S, Gondelaud F (2016) [Shuttling from the extracellular matrix to the nucleus]. Biol Aujourdhui **210**: 37-44.

Roberts S, Evans EH, Kletsas D, Jaffray DC, Eisenstein SM (2006) Senescence in human intervertebral discs. Eur Spine J **15**: 312-316.

Roughley PJ (2004) Biology of intervertebral disc aging and degeneration: involvement of the extracellular matrix. Spine (Phila Pa 1976) **29**: 2691-2699.

Sasarman F, Maftei C, Campeau PM, Brunel-Guitton C, Mitchell GA, Allard P (2016) Biosynthesis of glycosaminoglycans: associated disorders and biochemical tests. J Inherit Metab Dis **39**: 173-188.

Schrage YM, Hameetman L, Szuhai K, Cleton-Jansen A-M, Taminiau AHM, Hogendoorn PCW, Bovée JVMG (2009) Aberrant heparan sulfate proteoglycan localization, despite normal exostosin, in central chondrosarcoma. Am J Pathol **174**: 979-988.

Smith S, Melrose J. (2019) Type XI collagen-perlecan-HS interactions stabilise the pericellular matrix of annulus fibrosus cells and chondrocytes providing matrix stabilisation and homeostasis. J Mol Histol **50**: 285-294.

Smith SM, Shu C, Melrose J (2010) Comparative immunolocalisation of perlecan with collagen II and aggrecan in human foetal, newborn and adult ovine joint tissues demonstrates perlecan as an early

developmental chondrogenic marker. Histochem Cell Biol **134**: 251-263.

Song Y, Zhang F, Linhardt RJ. (2020) Analysis of the glycosaminoglycan chains of proteoglycans. J Histochem Cytochem 22155420937154. DOI: 10.1369/0022155420937154.

Stewart MD, Sanderson RD (2014) Heparan sulfate in the nucleus and its control of cellular functions. Matrix Biol **35**: 56-59.

Sun Q, Guo S, Wang CC, Sun X, Wang D, Xu N, Jin SF, Li KZ (2015) Cross-talk between TGF-β/Smad pathway and Wnt/β-catenin pathway in pathological scar formation. Int J Clin Exp Pathol **8**: 7631-7639.

Szirmai J (1969) Structure of Cartilage. In: Ageing of connective and skeletal tissue. (ed. Engle A, Larsson T), Nordiska Bokhandelns, Stockholm, pp 163-184.

Szirmai J (1974) The concept of the chondron as a biomechanical unit. In: Biopolymer und Biomechanik von Bindegewebssystemen. (ed. Hartmann F), Academic Press, Berlin-Heidelberg:New York, pp 87-91.

Tuzon CT, Rigueur D, Merrill AE (2019) Nuclear fibroblast growth factor receptor signaling in skeletal development and disease. Curr Osteoporos Rep **17**: 138-146.

Vertel B, Barkman LL (1984) Immunofluorescence studies of chondroitin sulfate proteoglycan biosynthesis: the use of monoclonal antibodies. Coll Relat Res **4**: 1-20.

Vertel B, Dorfman A (1978) An immunohistochemical study of extracellular matrix formation during chondrogenesis. Dev Biol **62**: 1-12.

Vertel B, Dorfman A (1979) Simultaneous localization of type II collagen and core protein of chondroitin sulfate proteoglycan in individual chondrocytes. Proc Natl Acad Sci U S A **76**: 1261-1264.

Vincent T, Saklatvala J (2006) Basic fibroblast growth factor: an extracellular mechanotransducer in articular cartilage? Biochem Soc Trans **34**: 456-457.

Vincent TL, McLean CJ, Full LE, Peston D, Saklatvala J (2007) FGF-2 is bound to perlecan in the pericellular matrix of articular cartilage, where it acts as a chondrocyte mechanotransducer. Osteoarthritis Cartilage **15**: 752-763.

Wang J, Markova D, Anderson DG, Zheng Z, Shapiro IM, Risbud MV (2011) TNF-α and IL-1β promote a disintegrin-like and metalloprotease with thrombospondin type I motif-5-mediated aggrecan degradation through syndecan-4 in intervertebral disc. J Biol Chem **286**: 39738-39749.

Wang JC (2002) Cellular roles of DNA topoisomerases: a molecular perspective. Nat Rev Mol Cell Biol **3**: 430-440.

Wang M, Tang D, Shu B, Wang B, Jin H, Hao S, Dresser KA, Shen J, Im HJ, Sampson ER, Rubery PT, Zuscik MJ, Schwarz EM, O'Keefe RJ, Wang Y, Chen D (2012) Conditional activation of β-catenin signaling in mice leads to severe defects in intervertebral disc tissue. Arthritis Rheum **64**: 2611-2623.

Whitelock J, Melrose J, Iozzo RV (2008) Diverse cell signaling events modulated by perlecan. Biochemistry **47**: 11174-11183.

Willert K, Nusse R (2012) Wnt proteins. Cold Spring Harb Perspect Biol **4**: a007864. DOI: 10.1101/cshperspect.a007864.

Willert K, Nusse R (1998) Beta-catenin: a key mediator of Wnt signaling. Curr Opin Genet Dev **8**: 95-102.

Wilusz R, Defrate LE, Guilak F (2012) A biomechanical role for perlecan in the pericellular matrix of articular cartilage. Matrix Biol **31**: 320-327.

Wilusz R, Sanchez-Adams J, Guilak F (2014) The structure and function of the pericellular matrix of articular cartilage. Matrix Biol **39**: 25-32.

Yang S, Liao Y, Zhao Q, Xie Y, Zheng A, Wan H (2018) Heparanase is a critical regulator of mitotic spindles required for maintaining chromosome stability. DNA Cell Biol 37: 291-297.

Youn I, Choi JB, Cao L, Setton LA, Guilak F (2006) Zonal variations in the three-dimensional morphology of the chondron measured *in situ* using confocal microscopy. Osteoarthritis Cartilage **14**: 889-897.

Yu J, Schollum ML, Wade KR, Broom ND, Urban JP (2015) ISSLS prize winner: a detailed examination of the elastic network leads to a new understanding of annulus fibrosus organization. Spine (Phila Pa 1976) **40**: 1149-1157.

Zhou B, Liu Y, Kahn M, Ann DK, Han A, Wang H, Nguyen C, Flodby P, Zhong Q, Krishnaveni MS, Liebler JM, Minoo P, Crandall ED, Borok Z (2012) Interactions between β-catenin and transforming growth factor-β signaling pathways mediate epithelial-mesenchymal transition and are dependent on the transcriptional co-activator cAMP-response element-binding protein (CREB)-binding protein (CBP). J Biol Chem **287**: 7026-7038.

Supplementary videos

Supplementary video 1. Available from paper webpage. Video depicting sequential images of perlecan immunolocalisations through the full depth of a string of AF cells (see Fig. 2 also).

Supplementary video 2. Available from paper webpage. Video depicting sequential images of perlecan immunolocalisations through the full depth of an NP cell (see Fig. 2 also).

Editor's note: There were no questions put to the authors, so there is no Discussion with Reviewers section for this paper. The Scientific Editor responsible for this paper was Sibylle Grad.